Cobalt tris(4-vinylphenyl)corrole: out of the frying pan into the polymer

Nicolas Desbois, W. Ryan Osterloh, Dimitri Sabat, Camille Monot, Stéphane Brandès, Michel Meyer, Capucine Chaar, Louise Hespel, Laurent Lebrun, Rachid Baati, et al.

Chemical Communications **2023**, *59*, 2098–2101 - DOI: 10.1039/d2cc06872a

Cobalt Tris(4-Vinylphenyl)Corrole: Out of the Frying Pan into the Polymer

Nicolas Desbois,[a] W. Ryan Osterloh,[a] Dimitri Sabat,[a] Camille Monot,[a] Stéphane Brandès,[a] Michel Meyer,[a] Capucine Chaar,[b] Louise Hespel,[c] Laurent Lebrun,[c] Rachid Baati,[d] François Estour*[b] and Claude P. Gros*[a]

[a] Université Bourgogne Franche-Comté, ICMUB, UMR CNRS 6302, 21078 Dijon Cedex, France. Email: claude.gros@u-bourgogne.fr
[b] Normandie Université, UNIROUEN, INSA Rouen, COBRA, UMR CNRS 6014, 76000 Rouen, France. Email : francois.estour@univ-rouen.fr
[c] Normandie Université, UNIROUEN, INSA Rouen, CNRS, PBS, 76000 Rouen, France
[d] Université de Strasbourg, ICPEES, UMR CNRS 7515, 67087 Strasbourg, France

A novel cobalt corrole bearing 4-vinylphenyl groups at the 5,10,15-*meso*-positions of the macrocycle has been synthesized from the tris(4-bromophenyl)corrole using a Suzuki coupling reaction. The spectral and electrochemical properties of this corrole are reported in CH_2Cl_2 along with its ability to form a highly stable six-coordinate complex and cross-linked corrole-based polymer in a 59% yield.

Corroles are aromatic, 23-atom tetrapyrrole macrocycles lacking one less *meso*-carbon atom as compared to their porphyrin congeners. Despite their structural similarity, trianionic corrole ligands lead to transition metal complexes showing significantly different properties than those of metalloporphyrins.[1] Given their rich chemistry and biological relevance, corroles and porphyrins are intensively used to form versatile molecules[2] and to mimic the function of biomacromolecules.[3] Furthermore, they are highly utilized in many chemical and photochemical processes as catalysts or photosensitizers.[4] In many cases, nature exploits the ability to alter the reactivity of a given protein by tuning the electronics of these essential macrocycles *via* changes in the central metal ion or structural modifications.[5] For this purpose, the development of systems with a macromolecular environment having a determining role, as is the case with the natural systems, is of great interest. In this context, numerous articles have been dedicated to the preparation of polymers involving porphyrins where synergistic effects have been shown to afford new targets with enhanced properties.[6] Indeed, the connectivity of porphyrin monomers influences the self-assembly of functional architectures and can provide efficient cooperative processes with polymers in various fields of applications,[7] especially in the degradation of toxics and contaminants.[8] In this regard, recent results on porphyrin-containing polymers showed high specificity for the detoxification of chemical warfare agents by using simulants.[9] Molecularly imprinted polymers have proved their particular advantage as a biomimetic heterogenous catalyst for the oxidation of sulphur derivatives involving vesicants and V nerve agent stimulants.[10] Compared to the many published examples involving porphyrin derivatives, literature on corrole-based polymers is much less abundant.[11] To address this, the current study focuses on the preparation, coordination and electrochemical properties of a polymerizable corrole monomer and its copolymerization with divinylbenzene.

Following optimized synthetic reports on the vinylation of aryl halides,[12] the free base tris(4-vinylphenyl)corrole (**$2H_3$**) was formed *via* a Suzuki-Miyaura cross-coupling reaction from the tris(4-bromophenyl)corrole precursor (**$1H_3$**) in a 41% yield (Scheme 1). This was then followed by a metalation reaction between **$2H_3$** and $Co(OAc)_2{\cdot}4H_2O$ to give the five-coordinate cobalt corrole, **2Co(DMSO)**, bearing *meso*-4-vinylphenyl groups at the 5,10,15-positions of the corrole macrocycle. The use of potassium vinyltrifluoroborate (CH_2CHBF_3K) was the preferred vinylating agent due to its reactivity.[12-13] Moreover, as opposed to generating the corrole *via* a direct route (*i.e.*, from pyrrole and 4-vinylbenzaldehyde) the vinylation of **$1H_3$** was found to result in a higher overall yield of **$2H_3$** (2.9% *vs* <1%).

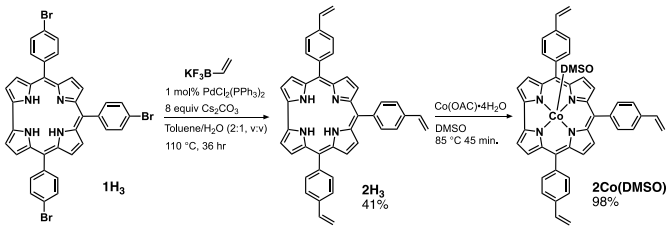

Scheme 1 Synthetic scheme for vinylation of **$1H_3$** to afford **$2H_3$** and the subsequent metalation reaction to generate the cobalt complex, **2Co(DMSO)**.

Characterization of **$2H_3$** and its cobalt complex was performed using ^{1}H NMR and UV-vis spectroscopy, ESI and MALDI-TOF mass spectrometry and, in the case of **2Co(DMSO)**, cyclic voltammetry (*vide infra*). The proton NMR spectrum of **$2H_3$** (see ESI† Fig. S7) displays typical signals for the eight β-pyrrole hydrogens appearing as four doublets between 8.3–9.0 ppm, and twelve *meso*-(*o*,*p*)-phenyl protons appearing as four doublets between 7.8–8.3 ppm with two resonances more intense than the other owing the symmetry of the corrole. In addition to these resonances, a splitting pattern characteristic of vinylic protons between 5.5–7.1 ppm is observed, where the most downfield shifted signal appears as doublet of doublets corresponding to the *cis*/*trans*-vicinal coupling[14] similar to what has been reported for related tetrapyrrole analogues.[10,15] A nearly identical splitting pattern is seen in the ^{1}H NMR spectrum of **2Co(DMSO)** recorded in ammonia-saturated $CDCl_3$ (see ESI† Fig. S10), in addition to a broad singlet at –6.7 ppm (6H) corresponding to the two coordinated NH_3 ligands.[16] The MALDI-TOF mass spectra (see ESI† Figs. S8 and S11) of both the free base and cobalt tris(4-vinylphenyl)corroles show minimal

fragmentation and base peaks located at *m*/*z* values consistent with their molecular formulation.[17]

Working towards the development of corrole-based molecularly imprinted polymers, this study focuses on the formation of a stable polymerization 'pre complex' comprised of the cobalt corrole bound to *N*-alkyl imidazole ligand(s) (**ImA**[18] in Fig. 1), a ligand which was previously employed as a template mimic of the nerve agent VX.[10] This imidazole-based template was chosen based on its steric demand, which closely reflects that of VX, as well as on previous studies, which have shown the enhanced ability of cobalt corroles to readily bind two nitrogen donor ligands in axial postions[16,19] and to release such ligands under mild acidic conditions.[20]

The ligand addition of **ImA** to **2Co(DMSO)** was monitored by both UV-vis absorption spectrophotometry in CH_2Cl_2 (Fig. 1) and by cyclic voltammetry in CH_2Cl_2/TBAP (Fig. 2). It is important to note that at the concentration level used for the UV-vis titrations (10^{-5} M), the labile **2Co(DMSO)** adduct dissociates, affording in solution only the four-coordinate cobalt corrole, denoted as **2Co**, as has been shown previously by concentration-dependent studies of structurally related compounds.[21] Moreover, the same studies have also confirmed that the DMSO ligand remains associated at the concentration (10^{-3} M) used for electrochemical measurements. As seen in Fig. 1, the UV-vis titration of **2Co** with the imidazole ligand template **ImA** involves an overall two-step process corresponding to the stepwise formation of the five- and six-coordinate species as depicted on the right side of the figure. The first step (Fig. 1a), associated with the decreased intensity of the Soret band at 395 nm and red-shift of the Q-band from 555 to 561 nm, is assigned as a conversion of **2Co** to **2Co(ImA)**. Confirmation of this assignment is provided by the diagnostic mole-ratio plot in the inset of Fig. 1. Upon further addition of **ImA** to the solution, a second spectral change is observed with notably different isosbestic points than those of the first. This second step, occurring at slightly higher concentrations of **ImA**, is associated with the loss of the Soret band at 399 nm and the appearance of new split Soret bands at 446 and 465 nm along with a concomitant increase of a sharp, intense Q-band at 640 nm; the latter of which is indicative of six-coordinate cobalt corroles.[16,19-20,21a,22] Thus, the second set of spectral changes reflects the formation of **2Co(ImA)$_2$**, the desired polymerization 'pre-complex'. A testament to the relatively high stability of this six-coordinate cobalt corrole as compared to pyridine[19a,19d,19f] or NH_3[16] bis-adducts is given by the fact that ~10 equivalents of **ImA** are needed to form **2Co(ImA)$_2$**. Further validation for the assigned ligand binding reactions is provided by the multiwavelength processing of two independent titration data sets by the nonlinear least-squares refinement program Hypspec 2014.[23] Factor analysis confirmed that no more than three absorbing species account for the observed spectral changes (see ESI† Fig. S1) and the computed log K_1 and log K_2 values for the first and second ligand addition steps were found to be 8.1(1) and 5.1(1), respectively (see ESI† for detailed information). The conversion of **2Co** to **2Co(ImA)$_2$** with only a small excess of ligand is notable, given previous studies on the binding of *N*-donor ligands to structurally related cobalt triarylcorroles have reported log K_2 values ranging from 1.1–3.9 for axial ligands such as pyridine[19a,19d,19f] or ammonia.[16] The refined values in the current study rival the log K_2 for cyanide anion binding, which range from 4.1–4.8 for a series of cobalt A_3-triaryl-corroles.[19e,21a] This observation is consistent with the increase in nucleophilicity of imidazole and *N*-alkylimidazole derivatives as compared to pyridine and ammonia,[24] as well as the fact that the nucleophilicity of *N*-alkylimidazoles increases with increasing length of the *N*-alkyl carbon chain.[25]

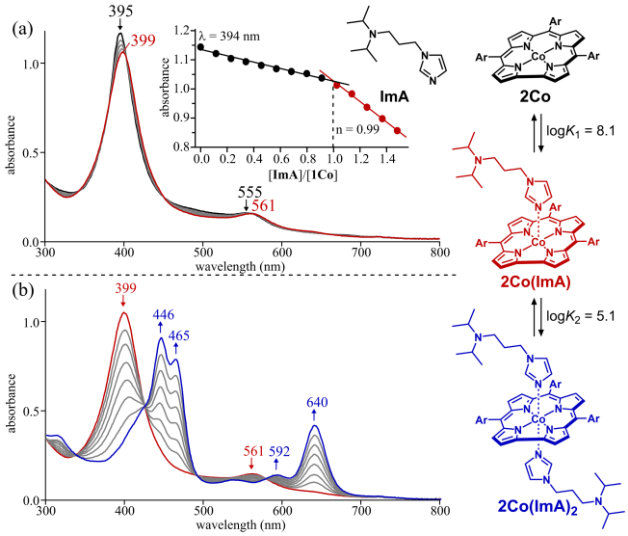

Fig. 1. UV-visible spectral changes of **2Co** in CH_2Cl_2 (at 10^{-5} M) upon the incremental addition of **ImA**, where (a) is the first step of the titration giving **2Co(ImA)** and (b) is the second step affording the six-coordinate species, **2Co(ImA)$_2$**. The inset in (a) shows the mole-ratio plot for the first ligand addition step. Ar = 4-vinylphenyl.

Further evidence showing formation of the polymerization 'pre-complex', **2Co(ImA)$_2$**, is given by the electrochemical titration data displayed in Fig. 2. The cyclic voltammograms prior to the addition of the ligand template (**ImA**) show **2Co(DMSO)** to be reversibly reduced at –0.14 V followed by a second irreversible reduction at E_{pc} = –1.66 V in CH_2Cl_2/0.1 M TBAP. On the basis of previous reports,[19e,21b] the first reversible reduction is coupled to the loss of the axial DMSO ligand and assigned to the generation of four-coordinate [**2Co**]$^-$, while the irreversible nature of the second electron addition is ascribed to a chemical reaction between the doubly reduced, four-coordinate cobalt corrole and the CH_2Cl_2 solvent.[26] An oxidative potential sweep reveals three stepwise one-electron oxidations of **2Co(DMSO)** at $E_{1/2}$ = 0.64, 0.81, and 1.45 V. Adding 1 mol equivalent of **ImA** to the solution results in a 520 mV cathodic shift in the first reduction (ΔE_{red}) and a 220 mV cathodic shift in the first oxidation (ΔE_{ox}), consistent with formation of **2Co(ImA)**. Moreover, in the presence of 1.0 mol equivalent of **ImA**, the irreversible second electron addition at E_{pc} = –1.66 V is constant, consistent with the transformation of five-coordinate **2Co(ImA)** to the four-coordinate form, [**2Co**]$^-$, at E_{pc} = –0.71 V following the first electron addition. Voltammograms obtained in the presence of 6.0 mol equivalents of **ImA** show a complete loss of current for the oxidation of **2Co(ImA)** at $E_{1/2}$ = 0.38 V and a concomitant appearance of new, cathodically shifted oxidation processes corresponding the **2Co(ImA)$_2$**. Under these solution conditions, the first and second oxidations are located at $E_{1/2}$ = 0.05 and 0.75 V, the first of which is shifted negatively by 330 mV with respect to the same process of **2Co(ImA)**.

Reductive scans of **2Co(ImA)$_2$** show a more complicated electron-transfer reaction.[27] Overall, the electroreductive behavior for the first reduction is consistent with an electrochemical-chemical (EC) 'box-mechanism' where the E_{pc} and E_{pa} values are separated on the basis a kinetically controlled step associated with the electron transfer, similar to that described for six-coordinate bis-Py and mono-CN cobalt corroles.[19d,19e] It is worth noting that the addition of excess **ImA** does not shift the first reversible oxidation process, further confirming formation of **2Co(ImA)$_2$** with <10 equivalents of **ImA**.

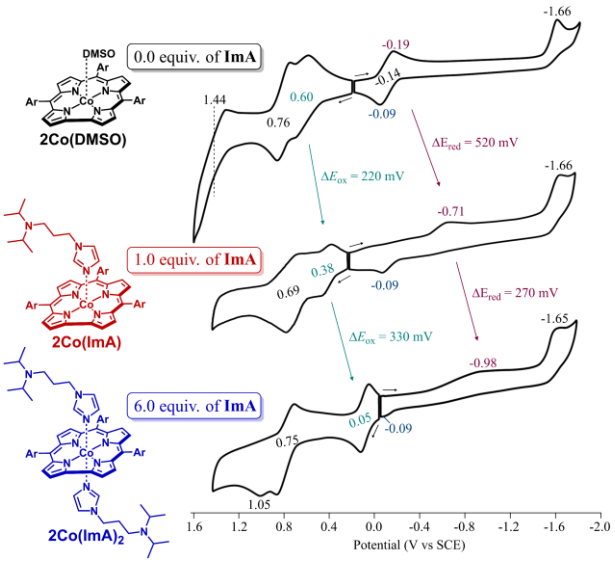

Fig. 2. Cyclic voltammograms of **2Co(DMSO)** in CH_2Cl_2/0.1 M TBAP containing a) 0, b) 1.0 and c) 6.0 equivalents of added **ImA**. Scan rate = 0.1 V/s. The coordination of the cobalt corrole under the given solution conditions is shown on the left.

Consistent with the information extrapolated from the UV-visible titration in Fig. 1, the observed shifts in redox potentials upon addition of **ImA** confirm the stepwise formation of **2Co(ImA)** and **2Co(ImA)$_2$**. The significant negative shift of the first electron abstraction (550 mV) and first electron addition (790 mV) upon going from **2Co(DMSO)** to **2Co(ImA)$_2$** demonstrates the enhanced ability of the *N*-alkyl imidazole template (**ImA**) to stabilize the higher oxidation state. Lastly, voltammograms of 10^{-3} M **ImA** in CH_2Cl_2/0.1 M TBAP show the ligand to be irreversibly oxidized at E_{pa} = 0.86 and 1.03 V (see Fig. S2) accounting for the '*extra*' anodic current associated with the second oxidation of **2Co(ImA)$_2$** and the additional peak at E_{pa} = 1.05 V (bottom of Fig. 2).

Having an efficient method of preparation and full characterization of **2Co(DMSO)**, an initial test was carried out to confirm the compounds' ability to form polymeric material. Polymerization was performed in anhydrous $CHCl_3$ containing a large excess of divinylbenzene (DVB, 500 equiv.) as a reticulating agent and 8 equiv. of the radical initiator, 2,2'-azo-bis-isobutyrylnitrile (AIBN). The vessel was sealed under an argon atmosphere and stirred at 65 °C for 18 hours. The resulting material was washed with $CHCl_3$, pulverized and passed through a 63 µm sieve giving the desired polymer in a 59% mass yield as green-dark powder while the control polymer formed using only DVB without **1Co(DMSO)** led to a white solid (Fig. 3a and 3b). A SEM analysis showed the morphology of polymer particles (Fig. 3c) and the confirmation for the incorporation of **2Co(DMSO)** into the resulting polymer was provided by ICP–MS analysis that revealed the presence of Co metal at a concentration of 926 µg g^{-1}. A TEM analysis proved the porous structure, with pore sizes ranging from a few nm to 100 nm, and particles of various shapes containing a homogeneous Co ion distribution in the volume (Fig. 3d).

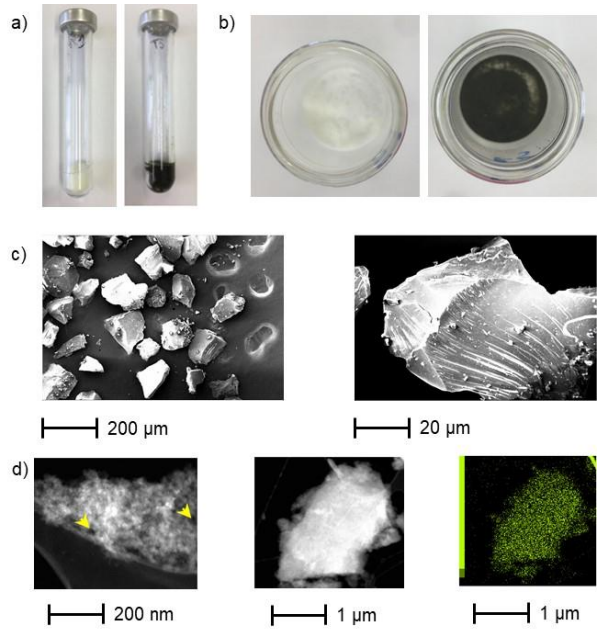

Fig. 3. Polymer characterization comparing (a) bulk polymers and (b) grinded and sieved polymers (pure DVB control polymer (white) *vs* **2Co(DMSO)** polymer (dark green)). SEM (c) and TEM (d) images of the **2Co(DMSO)** polymer.

In conclusion, we have developed a synthetic pathway to introduce polymerizable arms on a corrole scaffold *via* a Suzuki-Miyaura cross-coupling reaction. Cobalt insertion of the resulting tris(4-vinylphenyl)corrole gave a complex possessing tailored coordination and polymerization capabilities for potential use in a wide variety of materials akin to those based on porphyrins. This report paves a strategic approach for implementing new corrole-based Molecularly Imprinted Polymers (MIPs) as sensors (*e.g.*, carbon monoxide detection) or catalysts for process such as the oxygen reduction reaction. Moreover, the higher stability of the bis-ligated cobalt corrole 'pre-complex' as compared to the reported manganylporphyrin[10] (whose 'pre-complex' required 100 equiv. of **ImA**) should lead to an enhanced homogeneity during MIP formation leading to a more efficient functional material.

This work was supported by the Centre National de la Recherche Scientifique (CNRS) the Agence Nationale de la Recherche (ANR project MIPEnz-Decontam, grant n° ANR-20-CE39-0016, the Université Bourgogne Franche-Comté, and the Conseil Régional de Bourgogne. The authors thank the "Plateforme d'Analyse Chimique et de Synthèse Moléculaire de l'Université de Bourgogne" (PACSMUB, http://www.wpcm.fr) for providing access to spectroscopy instrumentation, Dr. Charles Devillers for access to the electrochemical equipment and Marie-José Penouilh and Dr. Quentin Bonnin (PACSMUB) for HRMS analyses. Mrs Sandrine Pacquelet (ICMUB) is warmly acknowledged for her synthetic contribution of corroles.

This work has also been partially supported by University of Rouen Normandy, INSA Rouen Normandy, European Regional Development Fund (ERDF), Labex SynOrg (ANR-11-LABX-0029), Carnot Institute I2 C, Labex EMC and Equipex Genesis program "Investissements d'avenir" ANR-11-EQPX-0020, the graduate school for research XL-Chem (ANR-18-EURE-0020 XL CHEM), and by Region Normandie. The authors from University of Rouen Normandy are grateful to Dr. Alexandra Pachéco-Bénichou for her contribution in the synthesis of polymeric materials and to Simona Moldovan from the Genesis platform - GPM laboratory (UMR 6634) for TEM analyses.

Conflicts of interest

The authors declare no competing financial interest.

Notes and references

1. J. F. B. Barata, M. G. P. M. S. Neves, M. A. F. Faustino, A. C. Tomé and J. A. S. Cavaleiro, *Chem. Rev.*, 2017, **117**, 3192-3253.
2. (a) M. Urbani, M. Grätzel, M. K. Nazeeruddin and T. Torres, *Chem. Rev.*, 2014, **114**, 12330-12396; (b) X. Zhang, M. C. Wasson, M. Shayan, E. K. Berdichevsky, J. Ricardo-Noordberg, Z. Singh, E. K. Papazyan, A. J. Castro, P. Marino, Z. Ajoyan, Z. Chen, T. Islamoglu, A. J. Howarth, Y. Liu, M. B. Majewski, M. J. Katz, J. E. Mondloch and O. K. Farha, *Coord. Chem. Rev.*, 2021, **429**, 213615; (c) C. Di Natale, C. P. Gros and R. Paolesse, *Chem. Soc. Rev.*, 2022, **51**, 1277-1335.
3. (a) C. J. Reedy and B. R. Gibney, *Chem. Rev.*, 2004, **104**, 617-650; (b) L. Flamigni and D. T. Gryko, *Chem. Soc. Rev.*, 2009, **38**, 1635-1646; (c) R. A. Baglia, J. P. T. Zaragoza and D. P. Goldberg, *Chem. Rev.*, 2017, **117**, 13320.
4. (a) Y.-M. Sun, X. Jiang, Z.-Y. Liu, L.-G. Liu, Y.-H. Liao, L. Zeng, Y. Ye and H.-Y. Liu, *Eur. J. Med. Chem.*, 2020, **208**, 112794; (b) H. Lei, X. Li, J. Meng, H. Zheng, W. Zhang and R. Cao, *ACS Catal.*, 2019, **9**, 4320-4344.
5. L. Zhao, R. Qu, A. Li, R. Ma and L. Shi, *Chem. Commun.*, 2016, **52**, 13543.
6. S. Frühbeißer and F. Gröhn, *J. Am. Chem. Soc.*, 2012, **134**, 14267-14270.
7. (a) E. Weyandt, L. Leanza, R. Capelli, G. M. Pavan, G. Vantomme and E. W. Meijer, *Nat. Commun.*, 2022, **13**, 248; (b) M. Li, Y. Zhang, X. Zhang, Z. Liu, J. Tang, M. Feng, B. Chen, D. Wu and J. Liu, *ACS Appl. Mater. Interfaces*, 2022, **14**, 48489-48501; (c) J. Wei, D. Wang, J. Li, J. Zhang, N. Wang and J. Li, *Appl. Organomet. Chem.*, 2022, **36**, e6820; (d) Q. Zha, X. Rui, T. Wei and Y. Xie, *CrystEngComm*, 2014, **16**, 7371-7384.
8. (a) L. Wang, J. Wang, Y. Wang, F. Zhou and J. Huang, *J. Hazard. Mater.*, 2022, **429**, 128303; (b) R. F. N. Quadrado, H. F. V. Vitoria, D. C. Ferreira, K. Krambrock, K. S. Moreira, T. A. L. Burgo, B. A. Iglesias and A. R. Fajardo, *J. Colloid Interface Sci.*, 2022, **613**, 461-476.
9. H. M. Choi, Y. J. Kim, E. T. Choi, T. Y. Lee and S. J. Lee, *J. Porphyrins Phthalocyanines*, 2022, **26**, 340-347.
10. S. Mohamed, S. Balieu, E. Petit, L. Galas, D. Schapman, J. Hardouin, R. Baati and F. Estour, *Chem. Commun.*, 2019, **55**, 13243-13246.
11. (a) A. Savoldelli, G. Magna, C. Di Natale, A. Catini, S. Nardis, F. R. Fronczek, K. M. Smith and R. Paolesse, *Chem. Eur. J.*, 2017, **23**, 14819-14826; (b) S. Brandès, V. Quesneau, O. Fonquernie, N. Desbois, V. Blondeau-Patissier and C. P. Gros, *Dalton Trans.*, 2019, **48**, 11651-11662; (c) Y. Zhao, Y. Peng, C. Shan, Z. Lu, L. Wojtas, Z. Zhang, B. Zhang, Y. Feng and S. Ma, *Nano Research*, 2022, **15**, 1145-1152; (d) H. Lei, Q. Zhang, Z. Liang, H. Guo, Y. Wang, H. Lv, X. Li, W. Zhang, U.-P. Apfel and R. Cao, *Angew. Chem. Int. Ed.*, 2022, **61**, e202201104; (e) A. Friedman, L. Landau, S. Gonen, Z. Gross and L. Elbaz, *ACS Catal.*, 2018, **8**, 5024-5031; (f) C. I. M. Santos, E. Oliveira, J. F. B. Barata, M. A. F. Faustino, J. A. S. Cavaleiro, M. G. P. M. S. Neves and C. Lodeiro, *J. Mater. Chem.*, 2012, **22**, 13811-13819.
12. G. A. Molander and A. R. Brown, *J. Org. Chem.*, 2006, **71**, 9681-9686.
13. G. A. Molander and N. Ellis, *Acc. Chem. Res.*, 2007, **40**, 275-286.
14. Gurudata, J. B. Stothers and J. D. Talman, *Can. J. Chem.*, 1967, **45**, 731.
15. (a) K. Kim, I. Kim, N. Maiti, S. J. Kwon, D. Bucella, O. A. Egorova, Y. S. Lee, J. Kwak and D. G. Churchill, *Polyhedron*, 2009, **28**, 2418-2430; (b) D. Khusnutdinova, M. Flores, A. M. Beiler and G. F. Moore, *Photosynthetica*, 2018, **56**, 67-74.
16. V. Quesneau, W. Shan, N. Desbois, S. Brandès, Y. Rousselin, M. Vanotti, V. Blondeau-Patissier, M. Naitana, P. Fleurat-Lessard, E. Van Caemelbecke, K. M. Kadish and C. P. Gros, *Eur. J. Inorg. Chem.*, 2018, **2018**, 4265-4277.
17. It should be noted that the base peak for **2Co(DMSO)** corresponds to $[M\text{-}DMSO]^+$ due to dissocation of the labile DMSO ligand.
18. **ImA** = 3-(*1H*-imidazol-1-yl)-*N*,*N*-diisopropylpropan-1-amine. This pseudo ligand template was synthezied and characterized as described in Ref. 10.
19. (a) K. M. Kadish, J. Shen, L. Frémond, P. Chen, M. El Ojaimi, M. Chkounda, C. P. Gros, J.-M. Barbe, K. Ohkubo, S. Fukuzumi and R. Guilard, *Inorg. Chem.*, 2008, **47**, 6726-6737; (b) K. M. Kadish, J. Shao, Z. Ou, C. P. Gros, F. Bolze, J.-M. Barbe and R. Guilard, *Inorg. Chem.*, 2003, **42**, 4062-4070; (c) S. Ganguly, J. Conradie, J. Bendix, K. J. Gagnon, L. J. McCormick and A. Ghosh, *J. Phys. Chem. A*, 2017, **121**, 9589-9598; (d) X. Jiang, M. L. Naitana, N. Desbois, V. Quesneau, S. Brandès, Y. Rousselin, W. Shan, W. R. Osterloh, V. Blondeau-Patissier, C. P. Gros and K. M. Kadish, *Inorg. Chem.*, 2018, **57**, 1226-1241; (e) W. R. Osterloh, N. Desbois, V. Quesneau, S. Brandès, P. Fleurat-Lessard, Y. Fang, V. Blondeau-Patissier, R. Paolesse, C. P. Gros and K. M. Kadish, *Inorg. Chem.*, 2020, **59**, 8562-8579; (f) N. I. Neuman, U. Albold, E. Ferretti, S. Chandra, S. Steinhauer, P. Rößner, F. Meyer, F. Doctorovich, S. E. Vaillard and B. Sarkar, *Inorg. Chem.*, 2020, **59**, 16622-16634.
20. (a) K. Sudhakar, A. Mahammed, N. Fridman and Z. Gross, *Dalton Trans.*, 2019, **48**, 4798-4810; (b) A. Mahammed, B. Mondal, A. Rana, A. Dey and Z. Gross, *Chem. Commun.*, 2014, **50**, 2725-2727; (c) A. Mahammed, M. Botoshansky and Z. Gross, *Dalton Trans.*, 2012, **41**, 10938-10940.
21. (a) W. R. Osterloh, V. Quesneau, N. Desbois, S. Brandès, W. Shan, V. Blondeau-Patissier, R. Paolesse, C. P. Gros and K. M. Kadish, *Inorg. Chem.*, 2020, **59**, 595-611; (b) X. Jiang, W. Shan, N. Desbois, V. Quesneau, S. Brandès, E. V. Caemelbecke, W. R. Osterloh, V. Blondeau-Patissier, C. P. Gros and K. M. Kadish, *New J. Chem.*, 2018, **42**, 8220-8229.
22. See also references listed in ESI – Section 1.2.
23. (a) P. Gans, A. Sabatini and A. Vacca, *Talanta*, 1996, **43**, 1739-1753; (b) http://www.hyperquad.co.uk/HypSpec2014.htm
24. J. R. Rumble, *Ed., CRC Handbook of Chemistry and Physics*, CRC Press/Taylor & Francis, Boca Raton, FL, 101 edn., 2020.
25. B. Lenarcik and P. Ojczenasz, *J. Heterocycl. Chem.*, 2002, **39**, 287-290.
26. (a) G. B. Maiya, B. C. Han and K. M. Kadish, *Langmuir*, 1989, **5**, 645-650; (b) X. Ke, R. Kumar, M. Sankar and K. M. Kadish, *Inorg. Chem.*, 2018, **57**, 1490-1503; (c) K. M. Kadish, X. Q. Lin and B. C. Han, *Inorg. Chem.*, 1987, **26**, 4161-4167; (d) K. M. Kadish, B. C. Han and A. Endo, *Inorg. Chem.*, 1991, **30**, 4502-4506.
27. As seen in Fig. 2, the initial negative potential sweep in the presence of 6.0 mol equiv. of **ImA** shows a first irreversible one-electron reduction at E_{pc} = –0.98 V *vs* SCE and is coupled to an anodic peak on the return potential sweep at E_{pa} = –0.09 V vs SCE. This latter value is identical to that observed for the same process prior to or after the addition of 1.0 equiv. **ImA** to solution, consistent with reoxidation of [**2Co**]$^-$ in each case.